



## TECHNICAL NOTE

D-414

### INSTRUMENTATION OF THE IONOSPHERE DIRECT MEASUREMENTS SATELLITE (EXPLORER VIII)

R. E. Bourdeau, J. L. Donley, and E. C. Whipple, Jr.  
Goddard Space Flight Center  
Greenbelt, Maryland

NATIONAL AERONAUTICS AND SPACE ADMINISTRATION  
WASHINGTON

April 1962

# INSTRUMENTATION OF THE IONOSPHERE DIRECT MEASUREMENTS SATELLITE (EXPLORER VIII)

by

R. E. Bourdeau, J. L. Donley, and E. C. Whipple, Jr.

*Goddard Space Flight Center*

## SUMMARY

This paper describes the ionosphere direct measurements satellite Explorer VIII, with emphasis on the physics of the experiments designed to measure electron density (RF impedance probe), electron temperature (electron temperature probe), positive ion concentration (ion current monitor), and ion mass (retarding potential probe). Experiments were also performed which measured the momentum, energy, and spatial distribution of dust particles. Experimental data presented is typical of that which has been processed to date.

The methods used by systems engineers to fulfill the special requirements imposed by the scientific experiments upon the overall satellite design are described; and data such as the satellite's thermal and spin-decay history are reported.

Of particular interest to spacecraft technologists concerned with the influence of the earth's magnetic field upon satellite orientation are the measurements on the effects of the potential differences at various points on the satellite surface. Finally, a new method for determining satellite aspect is introduced.

## CONTENTS

Summary . . . . .	i
INTRODUCTION . . . . .	1
LOCATION OF COMPONENTS . . . . .	4
THE EXPERIMENTS . . . . .	5
The RF Impedance Probe Experiment . . . . .	5
The Ion Current Monitor Experiment . . . . .	5
The Retarding Potential Experiment . . . . .	10
The Two-Element Electron Temperature Experiment . . . . .	12
The Three-Element Electron Temperature Experiment . . . . .	14
The Electron Current Monitor Experiment . . . . .	14
The Total Current Monitor Experiment . . . . .	18
The Micrometeorite Experiments . . . . .	18
The Electric Field Meter Experiment . . . . .	20
DESCRIPTION OF THE INSTRUMENTATION . . . . .	21
MECHANICAL SYSTEMS . . . . .	26
SOME RESULTS RELATED TO SPACECRAFT TECHNOLOGY . . . . .	28
ENVIRONMENTAL TESTING . . . . .	32
ACKNOWLEDGMENTS . . . . .	33
References . . . . .	34

# INSTRUMENTATION OF THE IONOSPHERE DIRECT MEASUREMENTS SATELLITE (EXPLORER VIII)\*

by

R. E. Bourdeau, J. L. Donley, and E. C. Whipple, Jr.

*Goddard Space Flight Center*

## INTRODUCTION

The Ionosphere Direct Measurements Satellite, Explorer VIII (1960  $\xi$ ), was launched by a Juno II vehicle (Figure 1) from Cape Canaveral, Florida, on November 3, 1960, into an orbit with an inclination of 50 degrees, a perigee height of 425 kilometers, and an apogee height of 2300 kilometers. Its planned active life was two months.

The primary mission of Explorer VIII was to acquire data on charged particles with thermal energies, a group which exerts great influence on communications. As the name further implies, the measurements were made by techniques which depend on sampling the spacecraft's local environment, with data transmitted to the earth over the telemetry link. Thus, the satellite differs from other U.S. ionosphere satellites, in which the ionospheric parameters have been obtained indirectly by means of ground-based observations of the arrival characteristics of satellite radio signals.

The ionospheric parameters measured by Explorer VIII were the electron concentration  $N_e$ , the electron temperature  $T_e$ , the positive ion concentration  $N_+$ , and the positive ion mass  $M_+$ . These data were obtained by five separate experiments, two being used for the electron temperature measurements.

A body moving at a high velocity through an ionized medium modifies the characteristics of the medium, and the extent of modification caused by Explorer VIII had to be known in order to derive meaningful geophysical quantities from the ionospheric experiments. Specifically, it was deemed important to know the behavior of four quantities as functions of the spacecraft orientation relative to velocity, magnetic field, and solar vectors. These quantities were: (a) the potential  $\phi$  which develops between the satellite and the medium as a result of their interaction; (b) the electron current ( $i_e$ ), flowing from

\*Presented at the American Rocket Society-Institute of Aeronautical Sciences joint meeting, Los Angeles, California, June 1961.

the medium to the satellite; (c) the positive ion current  $(i_+)_s$  also flowing from the medium to the satellite; and (d) the current  $(i_p)_s$  due to the photoemission of electrons from the satellite surfaces as a result of solar radiation. The subscript "s" indicates the values for current as observed at the skin of the spacecraft. As it happened, the measurement of these four quantities, which required the five geophysical experiments mentioned plus two additional experiments, made it possible to develop a model of the plasma sheath which formed around the satellite. Table 1 lists these seven experiments.

D-414

Table 1  
Explorer VIII Experiments Used for Ion Sheath Model

Experiment	Ionospheric Parameter	Sheath Parameter
1. RF impedance probe	$N_e$	
2. Ion current monitor	$N_+$	$(i_+)_s$
3. Retarding potential probe	$M_+$	
4. Two-element electron temperature probe	$T_e$	$(i_e)_s, \phi$
5. Three-element electron temperature probe	$T_e$	$\phi$
6. Electron current monitor		$(i_e)_s + (i_p)_s$
7. Total current monitor		$(i_e)_s + (i_+)_s + (i_p)_s$

Because it was estimated before launch that the orders of magnitude of the ion, electron, and photoemission currents would be comparable, it was decided that they should be measured separately, if possible. In particular, experience with Langmuir probes has shown that, in rockets where the ion and electron currents were not separated, uncertainties exist in the measured electron temperatures. For such reasons, five of the six current sensors (Experiments 2 - 7) were constructed so as to perform the separation of currents in situ, while the sixth current sensor measured the net or total current to a representative satellite area. The latter served both as a check on the other sensors and as a calibration monitor.

## THE EXPERIMENTS

### The RF Impedance Probe Experiment

The objective of the RF impedance probe experiment was to measure electron concentration. This was accomplished by comparing the inflight capacitance  $C$  of the sensor with its free-space value  $C_0$ . The value of  $C_0$  was measured before flight by the use of one of the two antenna wires and a half shell which was fabricated to the satellite configuration. The cut was made through the spin-axis and the half-shell was then placed on the appropriate ground plane. This experiment had been tested previously in vertical sounding rockets (Reference 1).

Electron concentration could be computed from the Appleton-Hartree formula which relates  $N_e$  to the dielectric constant  $K$  of the medium:

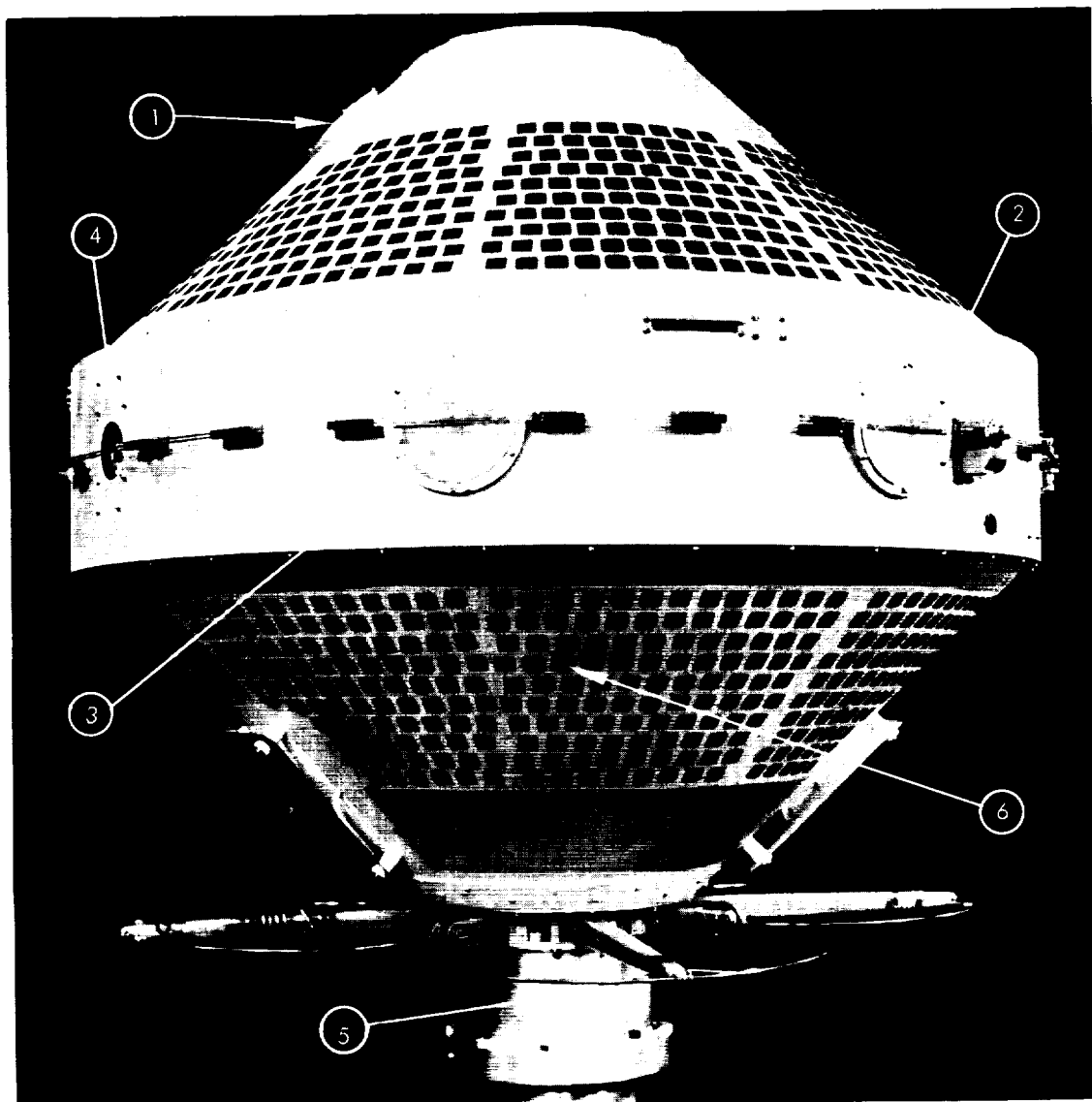
$$K = \frac{C}{C_0} = 1 - \frac{81 N_e}{f^2} \quad (1)$$

where  $f$  is the frequency (6.5 Mc) of the voltage applied to the antenna probe. It should be emphasized that the radiated power was negligibly small.

Since  $C_0$  was measured before flight and  $f$  was known, it was necessary to measure only  $C$  in order to compute  $N_e$ . The method used to measure  $C$  is illustrated schematically in Figure 5. The heart of the system was an oscillator whose frequency was determined in part by a sweep generator and in part by the capacitance of the aforementioned sensor. The start of the sweep was triggered by an 80-millisecond square wave developed from a gate in the telemetry system. A crystal filter delivered an output pulse to the computer each time the oscillator was tuned to 6.5 Mc. Two such pulses occurred every 80 milliseconds because the sweep generator output has an up and a down sweep. The time intervals between the start of the sweep and the occurrence of the two pulses were a measure of the probe capacitance. These intervals were presented to the telemetry system by the computer, in digital form. Since  $C$  was measured every 40 milliseconds, the experiment could, in principle, search out ionospheric heterogeneities with dimensions as small as 300 meters.

### The Ion Current Monitor Experiment

The geophysical objective of the ion current monitor experiment (Figure 6) was to measure positive ion concentrations. The sensor, constructed in planar geometry, consisted of three parallel electrodes. The outer grid was flush with and electrically connected to the satellite skin, acting as an electrostatic shield and preventing potentials on the inner electrode from disturbing the plasma sheath that surrounds the satellite. The inner grid was biased negatively to remove incoming electron current and to suppress photoemission from the collector. Consequently, the collector current  $i_+$  contained only the contribution of positive ions.



- ① Three-element electron temperature probe;
- ② Ion current monitor;
- ③ Retarding potential probe;
- ④ Micrometeorite photomultiplier;
- ⑤ Telemetry antenna;
- ⑥ Thermal coatings

Figure 3 - Explorer VIII satellite turned 180 degrees from Figure 2, showing additional component locations

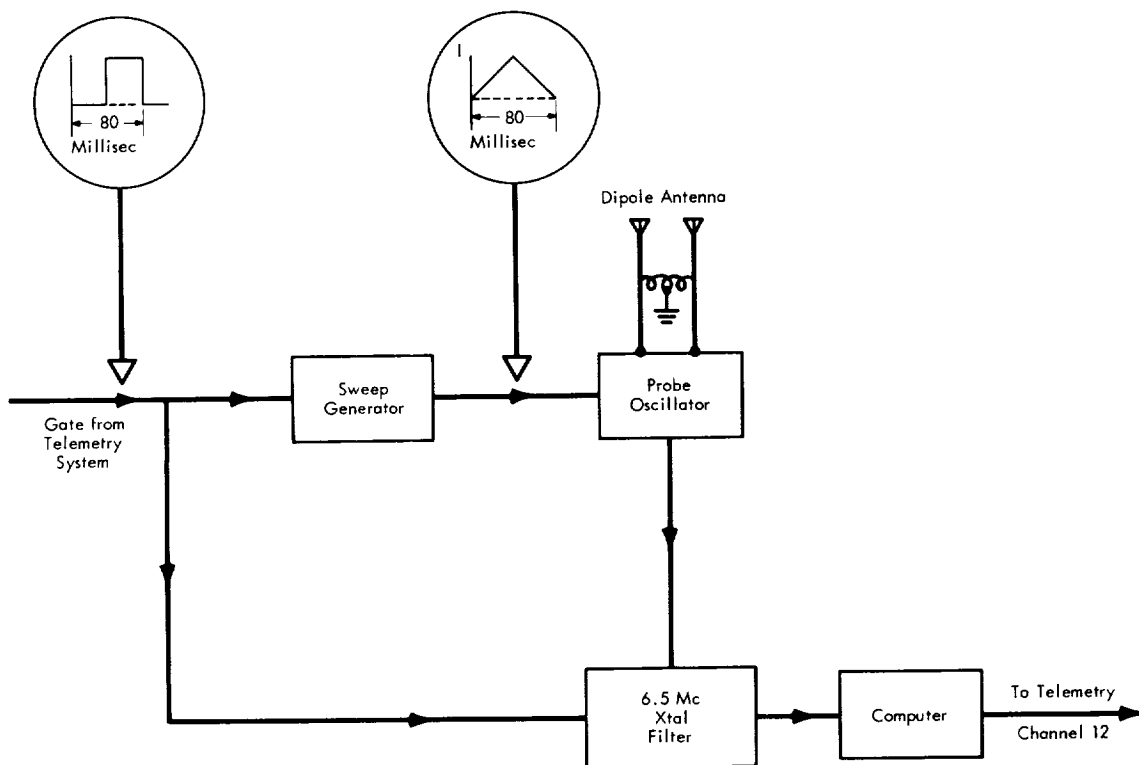


Figure 5 - The RF impedance probe experiment

Because of weight limitations, operation of the electrometer was time shared with the retarding potential experiment and the two-element electron temperature probe experiment by means of a mechanical commutator. One of the commutator switches connected the electrometer input to the collector of the ion current monitor (at point A in Figure 6) for 30 seconds of each 90-second interval. At the same time another switch (at point C) connected the electrometer return and the shield braid of the coaxial cable to the satellite potential. During each 30-second interval, a third switch (at point B) changed the system sensitivity in three steps of 10 seconds each by successive application of three separate collector load resistors. Such a range switch was necessary because the ion concentration could change from  $10^6/\text{cm}^3$  at perigee to  $10^3/\text{cm}^3$  at apogee.

The electrometer uses 100 percent feedback — a feature which provides the system with important characteristics. First, it insures long term stability: Less than one percent drift was observed when the system was tested for two weeks in a vacuum, while the package temperature was cycled between  $0^\circ$  and  $50^\circ$  C. Second, feedback keeps the collector at the satellite potential, irrespective of the voltage drop across the collector load resistor. Third, the feedback permits the sensor to be at a distance from the mechanical commutator and the electrometer. This is because it brings about an "effective" short



D-414

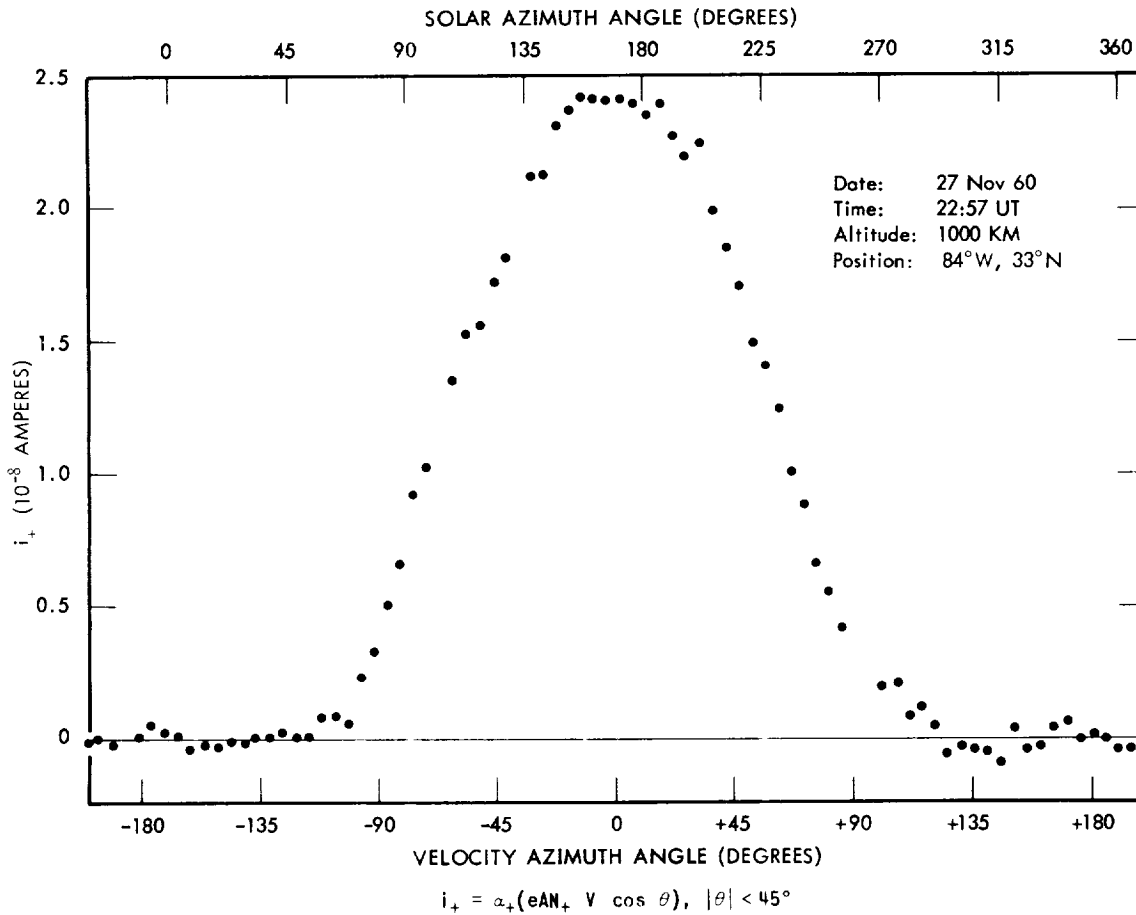


Figure 7 - Ion current as a function of aspect

with the ion current monitor experiment and the two-element electron temperature probe experiments, each experiment being on for 30 seconds during each 90-second interval. Just as in the case of the ion current monitor, the electrometer had three sensitivity ranges, each lasting for 10 seconds. The retarding potential was applied at the electrometer return and to the shield braid by a switch located at point C.

Figure 9 shows an actual volt-ampere curve taken during the flight of Explorer VIII. Since the satellite travels much faster than the positive ions, the ions have a kinetic energy, relative to the satellite, which is proportional to their mass. Specifically, the collector potential (relative to the plasma) required to retard half the ions of a given mass is

$$\phi_{cp} = \phi_{cs} + \phi = \frac{M_+ (V \cos \theta)^2}{2e}, \tag{3}$$

D-414

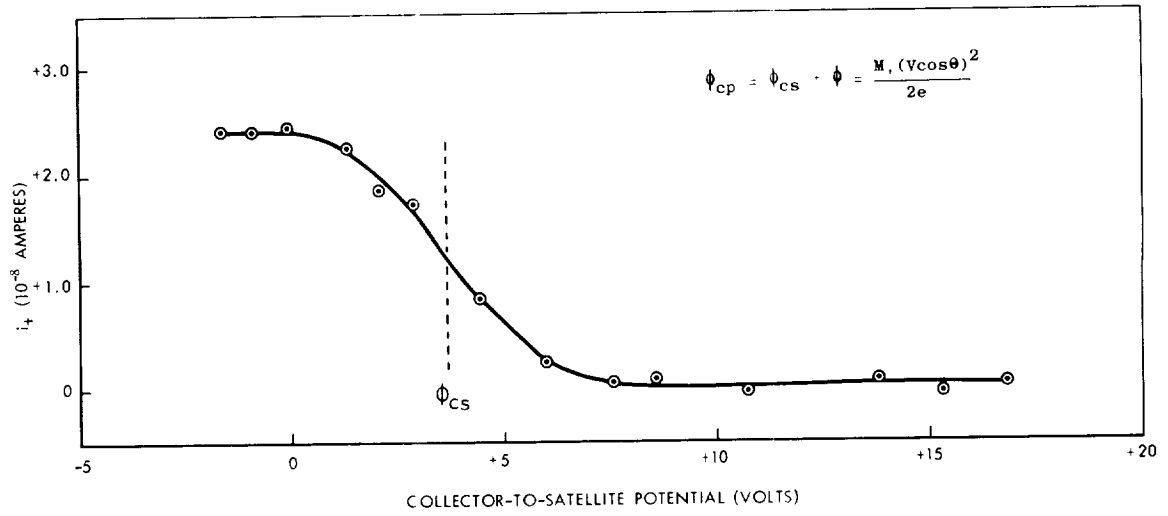


Figure 9 - Typical volt-ampere curve for retarding potential experiment

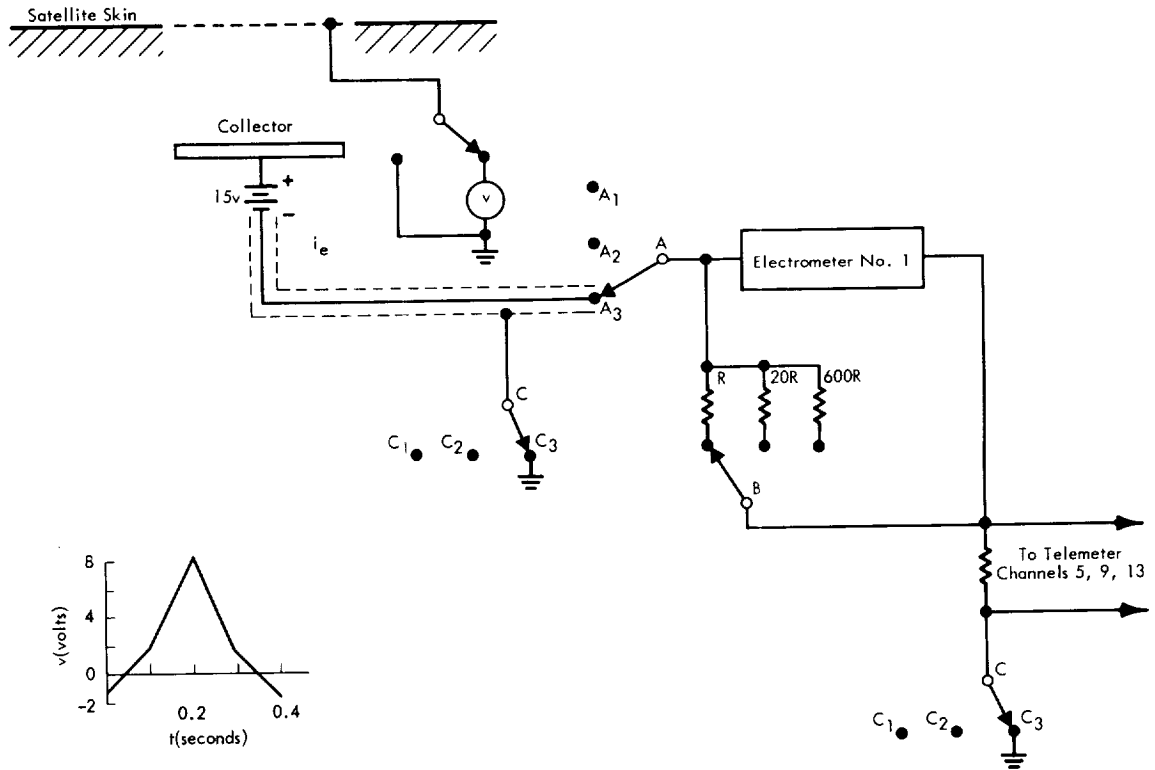


Figure 10 - The two-element electron temperature probe

D-414

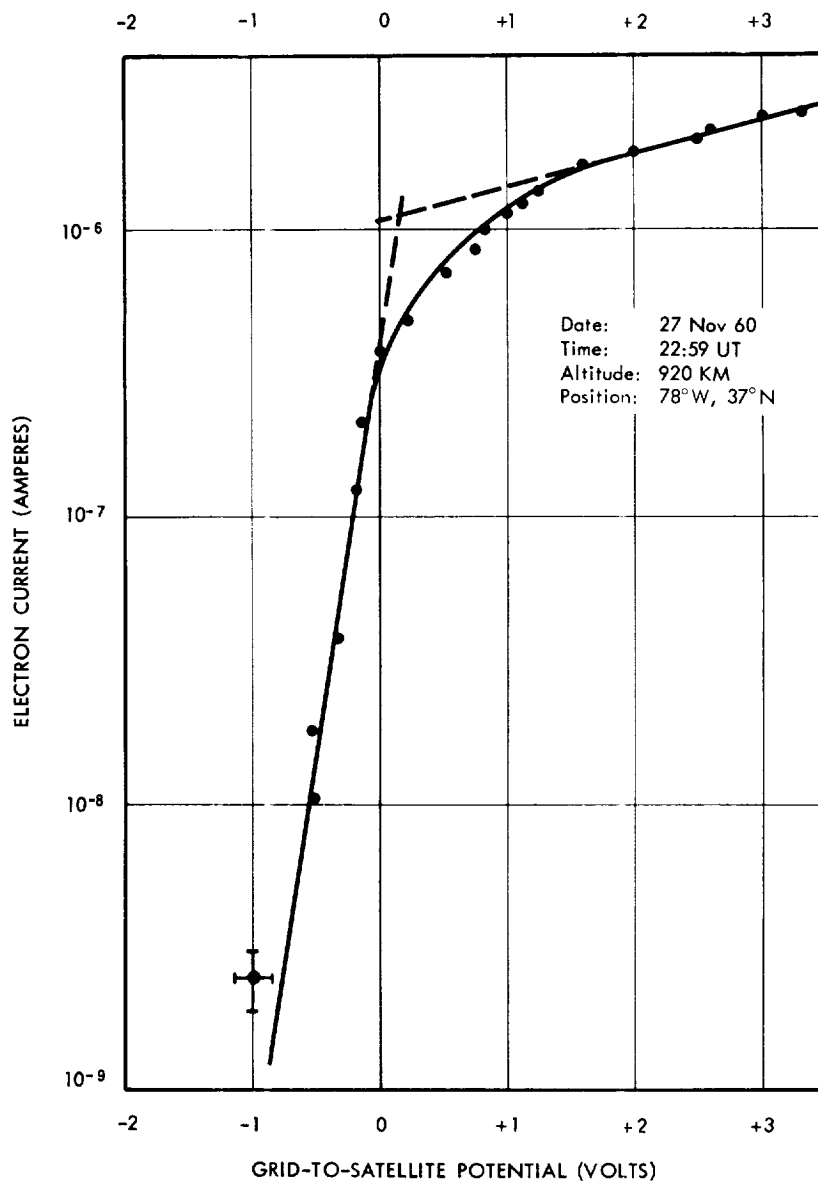


Figure 11 - Typical volt-ampere curve for the two-element electron temperature probe. The dashed lines are extrapolations indicating the angle of intersection between the part of curve below plasma potential with that above plasma potential.

the measured collector current. In this case, the collector current contained contributions from both the incoming electron current and photoemission and was

$$i = \alpha_e (i_e)_s + \alpha_p (i_p)_s, \quad (4)$$

where  $\alpha_e$  and  $\alpha_p$  are the respective grid transparencies.

D-414

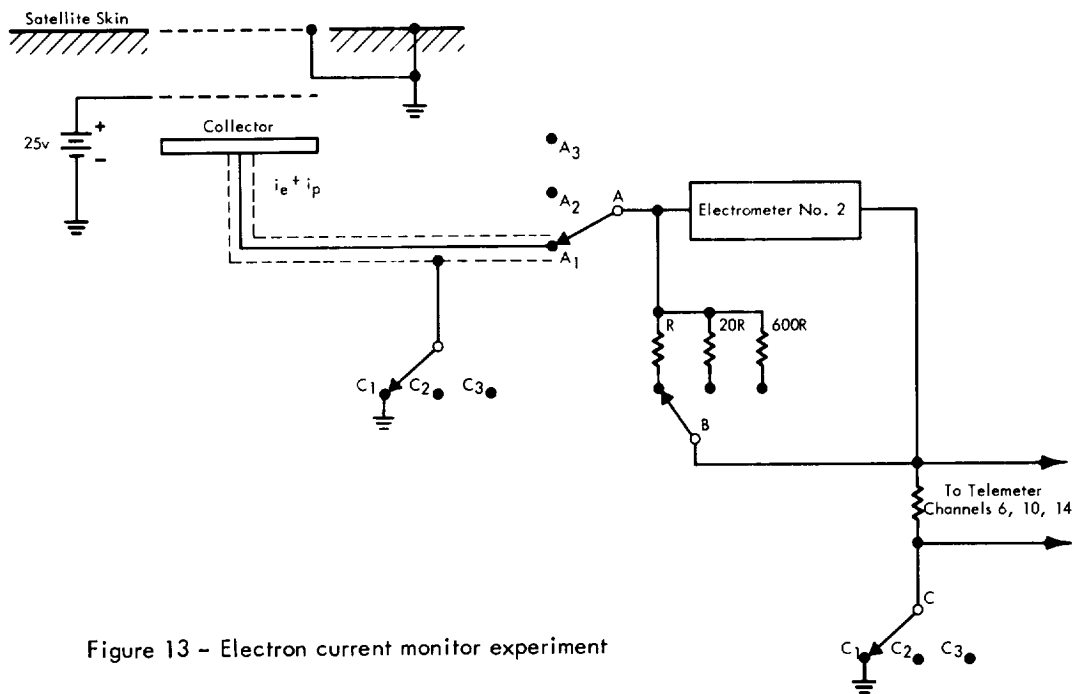


Figure 13 - Electron current monitor experiment

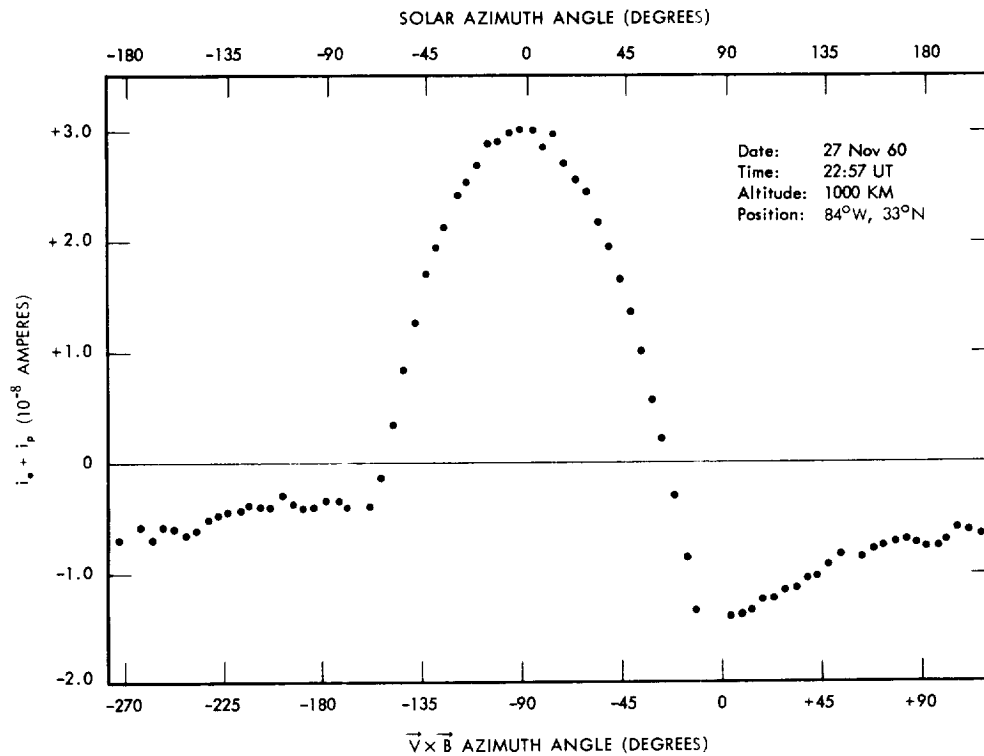


Figure 14 - Electron current as a function of aspect

D-414

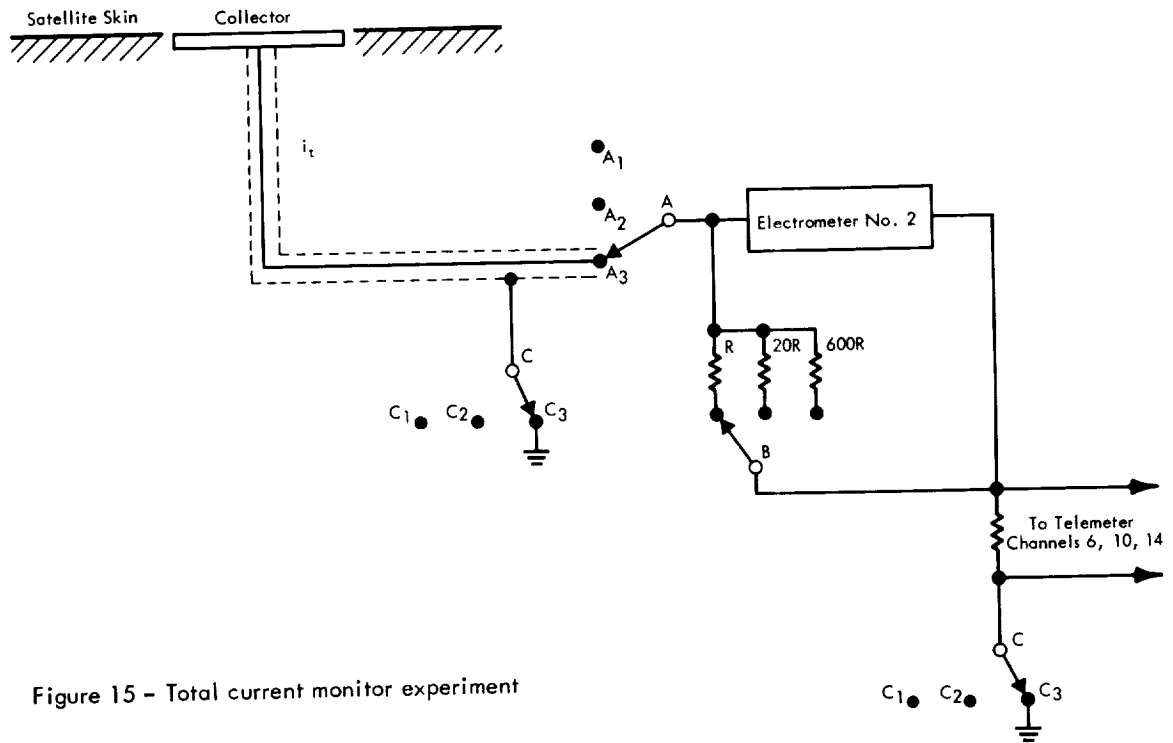


Figure 15 - Total current monitor experiment

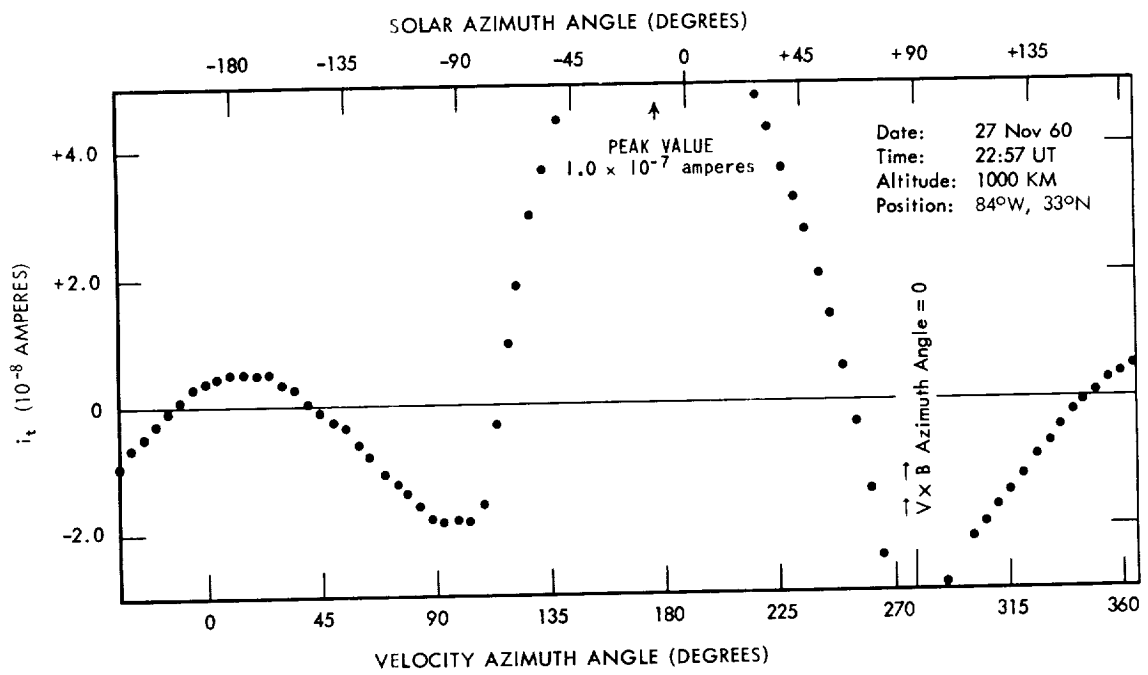


Figure 16 - Total sheath current as a function of aspect

where  $\epsilon$  is a constant,  $A$  is the stator area,  $\omega$  is the angular rotor frequency,  $R$  is the stator resistive load, and  $J$  is the net diffusion current density.

As will be seen from Figure 18, a synchronous wave is developed at the back end of the sensor. This signal is used by the motor control servo and the synchronous rectifier to measure  $V_E$ . The total output is

$$V_T = \sqrt{V_E^2 + V_J^2} \quad (8)$$

This experiment will measure fields as high as 10,000 volts/meter with a noise equivalent of less than 10 volts/meter. The residual field drift due to rotor-to-stator contact potential is also less than 10 volts/meter. The exposed surfaces of the field meter are gold plated and the rotor-to-stator spacing is 3 millimeters.

Because of the large power demand (3 watts) and the limited mechanical lifetime of the driving motor, the experiment was turned on by command from the ground. During the "on" time the outputs were time shared into the telemetry system by the mechanical commutator. After two minutes of operation, the experiment was automatically turned off by a command program module.

## DESCRIPTION OF THE INSTRUMENTATION

Only a small percentage of the weight of Explorer VIII could be devoted to actual instrumentation. The weight distribution of the major systems is listed in Table 2.

Table 2  
Weight of the Major Systems in Explorer VIII

System	Weight (lb)
Structure and mechanical systems	34
Batteries	34
Wiring and connectors	3
Sensors	5
Instrumentation	12

The instrumentation column of the satellite is shown in Figure 19. The supporting instrumentation includes a separation timer, aspect instrumentation, computers, a telemetry system and transmitter, and a command receiver. Considerable planning was

D-414

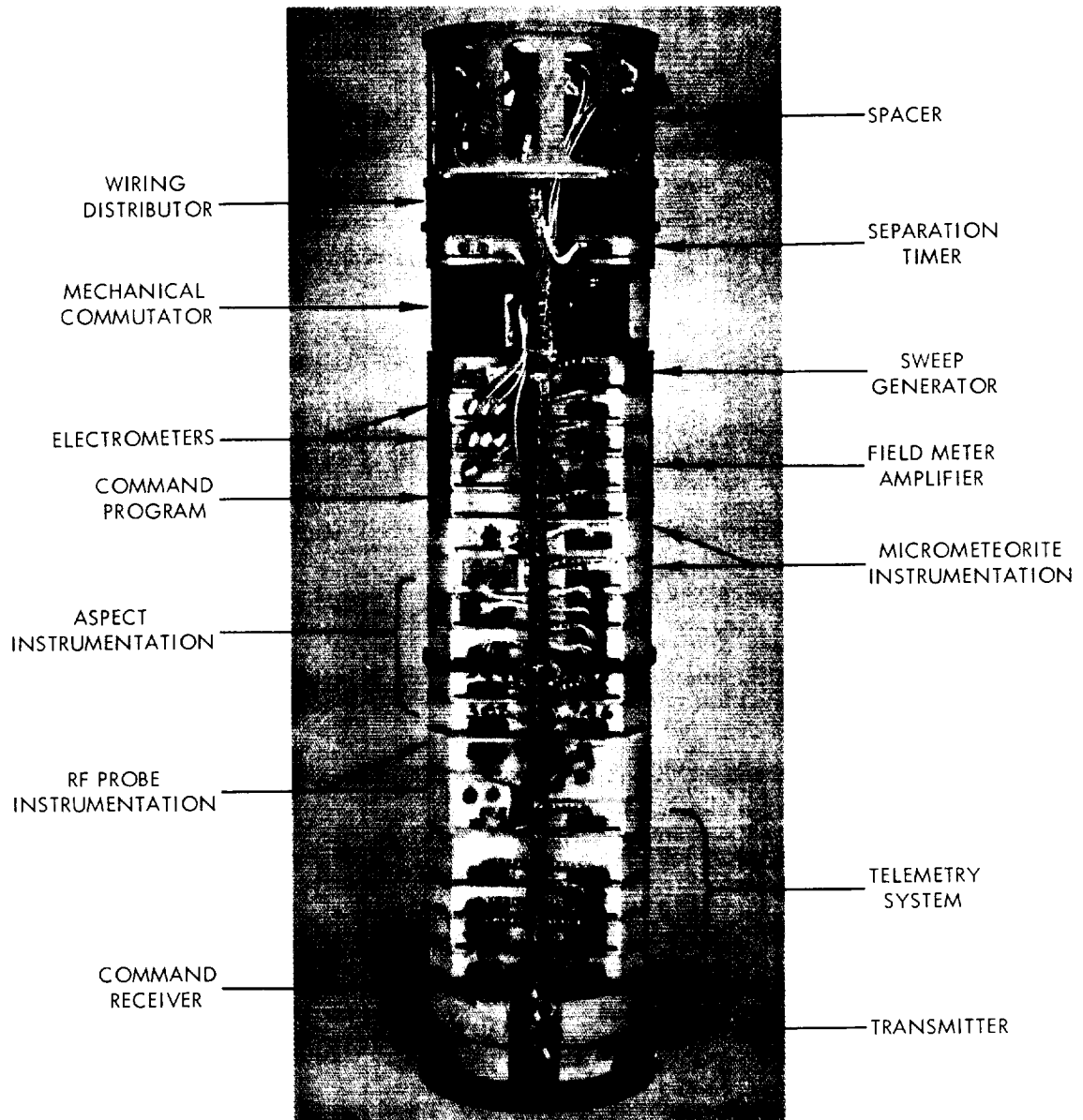


Figure 19 - Instrumentation column

volts applied to the two-element electron temperature probe experiment (Figure 10); and (3) a telemetered output at two volts. A low output impedance (10K ohms) was used in order to prevent the current flowing out of the medium from affecting the pertinent electrode potentials.

D-414

The aspect system used in Explorer VIII was a combination solar and horizon sensing unit. The solar portion consisted of two slits, behind each of which was placed a photo-sensitive silicon diode. One slit was parallel to the spin axis and the other was slanted approximately 25 degrees from it. The horizon portion consisted of two diodes located behind small, appropriately located apertures. The horizon and solar sensors shared common instrumentation which measured the time of an indication to within five milliseconds. The source of the indication was identified by the magnitude of the signal received by the pertinent diode. Measurement of the time between indications on the two solar slits, when compared to the roll period, permits calculation of the angle between the sun vector and the spin axis. The angle between the spin axis and the satellite position vector may be obtained from horizon indications in a similar manner. The overall aspect system was designed to determine satellite orientation to an accuracy of one degree.

The data telemetry system operated continuously, so all data transmission was in real time. This system is a descendant of the one used in the Vanguard satellites. The transmitter output contains bursts of amplitude modulation separated by periods of no oscillation (blanks). The frequency within each tone burst was varied from 9 to 22.5 kc in either an analog or a digital (eight discrete frequencies) form. The length of the blanks was varied between 0.5 and 1.1 milliseconds. The average radiated power at 108 Mc was 100 milliwatts. For data acquisition, the required predetection receiver bandwidth was 50 kc. For this value, at a 1500-mile range and with a receiver antenna gain of 18 db, the predicted signal-to-noise ratio of 14 db was obtained.

The basic element of time in the telemetry system, called a frame, is approximately 40 milliseconds long and contains sixteen alternate bursts and blanks, with the sixteenth burst longer than the other bursts. This provides a means of synchronization to identify the start of a frame. Table 4 gives the telemetry allocations for each frame and identifies the bursts as digital or analog. The temperature at four separate locations on the payload was telemetered by means of four variable-length blanks.

Upon the introduction of an appropriate signal from the command transmitter, the command receiver in conjunction with the command program module turned on the electric field meter, then turned it off after a two-minute interval. Except for the electric field meter experiment, all instrumentation operated continuously.

The chemical power supply on Explorer VIII was allotted to the satellite in such a way that the scientific experiments and the RF transmissions would terminate as closely



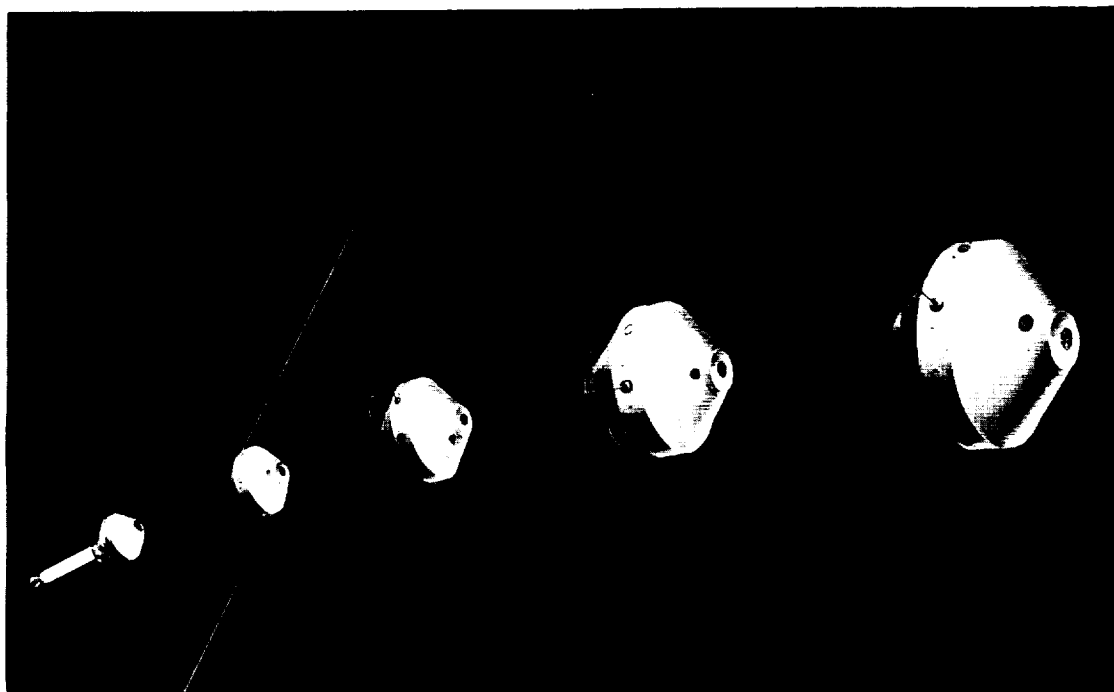


Figure 20 - The orbital injection sequence of Explorer VIII

unfavorable moment of inertia with the fourth-stage bottle attached. The squib-fired first-phase despin procedure consisted of extending and discarding two weighted wires which were originally wrapped around the equator of the satellite. This phase was designed to decrease the payload spin rate from the launch value of 450 rpm to about 100 rpm. Release of the wires from the payload initiated the extension, by centrifugal action, of the RF impedance probe, which simultaneously served to provide the second phase of despin. The probe consisted of two 10-foot flexible wires, weighted at the ends. Prior to deployment the wires were stored on a spool within the payload. The rate of extension was held to a speed of 1 foot per second by means of a mechanical brake arrangement. The final orbital spin rate of 22.1 rpm was well within the overall design criteria. This rate had decayed only to 21.4 rpm at the end of one month.

The satellite was designed to maintain stability about its spin axis. Favorable moments of inertia were obtained by locating the batteries near the periphery of the payload; thus the moment of inertia about the spin axis was 25.95 in-lb-sec<sup>2</sup>, whereas the maximum and minimum transverse moments of inertia were 20.89 and 19.11 in-lb-sec<sup>2</sup>.

D-414

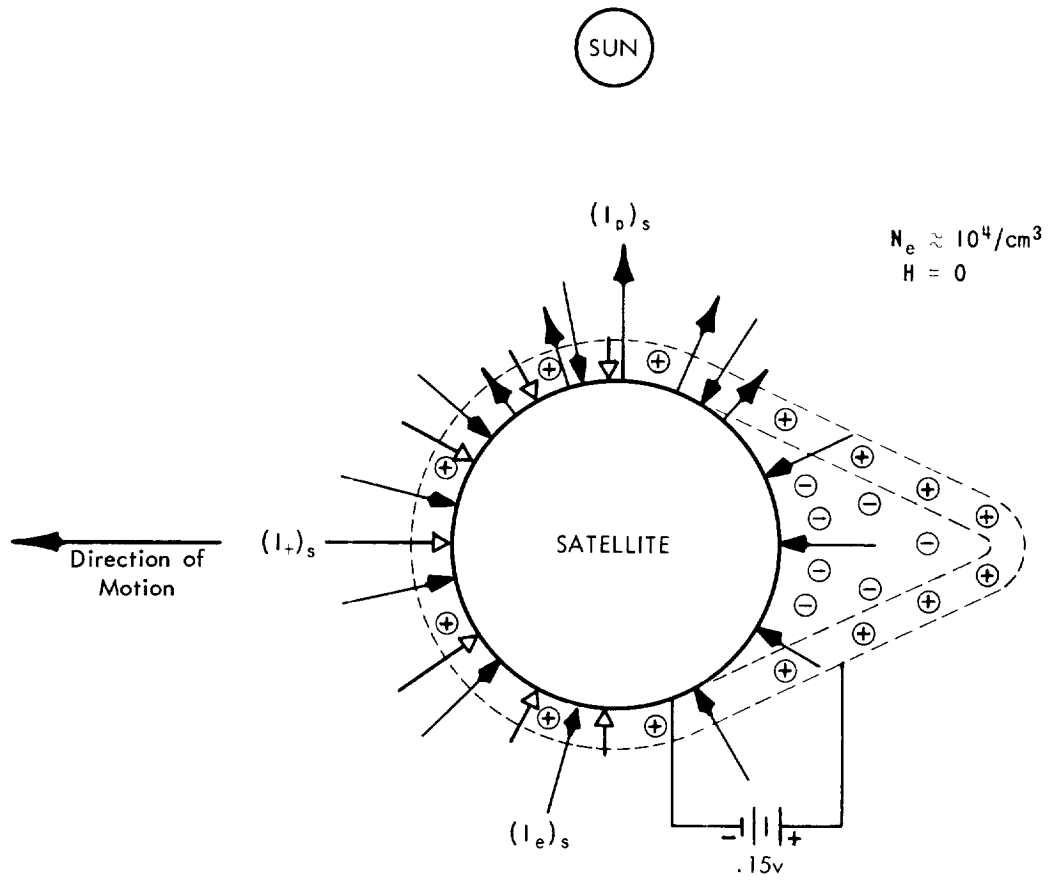


Figure 21 - Qualitative Explorer VIII sheath model postulated from experimental data

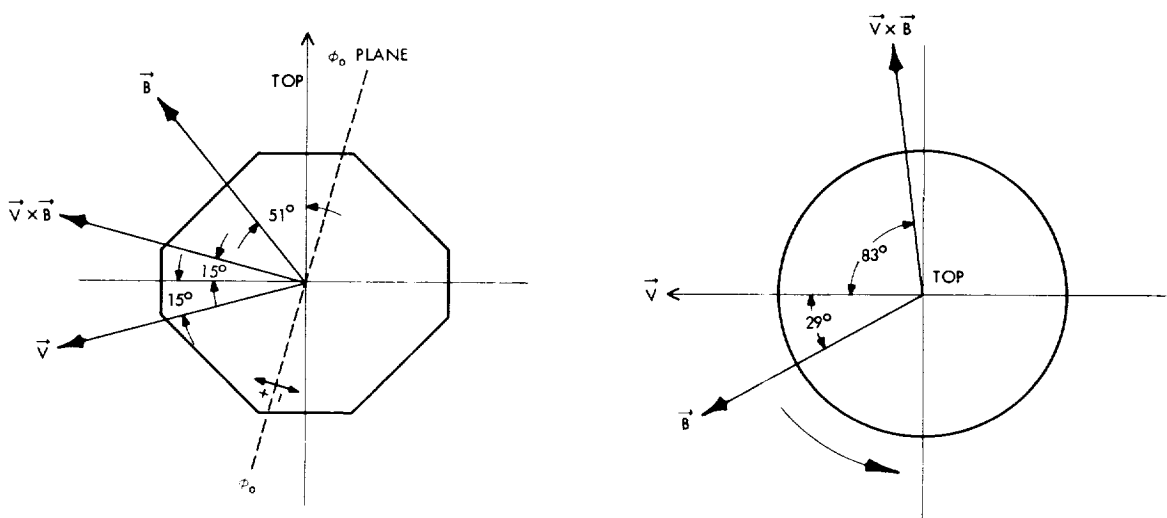


Figure 22 - Orientation of Explorer VIII with respect to magnetic field and velocity vectors

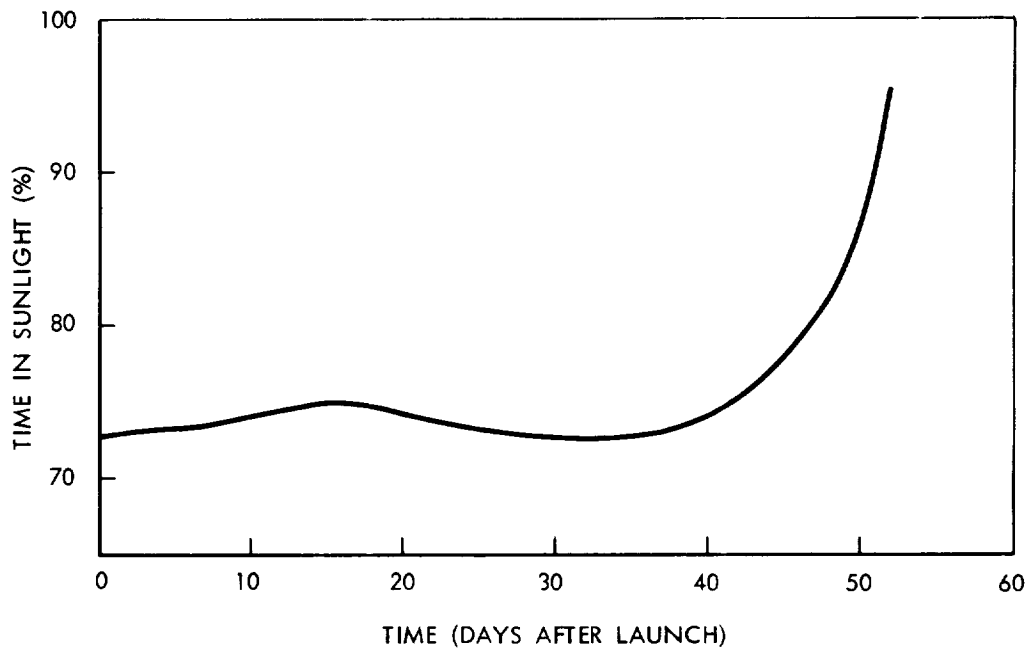
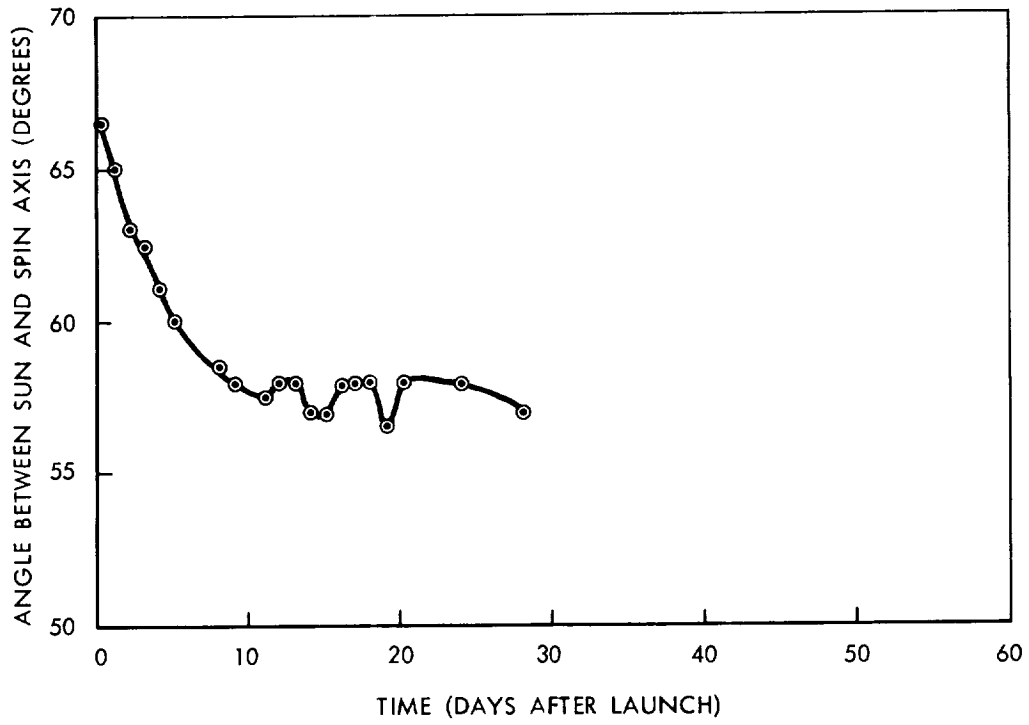


Figure 23 - Explorer VIII solar orientation

vibration first rather than the parallel operation used in the Explorer VIII prototype testing. Thus a single prototype can be used in place of the electric and environmental prototypes.

Second, it was found that quality control on surface emissivity was difficult to maintain from one model to another. This makes the need for a thermal prototype questionable. It is felt that data permitting a rough design for thermal control can be used while the single prototype mentioned above is undergoing vacuum temperature tests. Final touching up could then be made from data obtained on the actual flight model.

Third, it was found that a more reliable and expedient method of handling the flight models would be to eliminate one and depend upon spare components. In this manner, more attention could be paid to the single flight unit and rarely would a replacement part have to be used.

A recommended test program for future use, based on experience with Explorer VIII, is as follows: First, test and evaluation personnel should determine, by actual measurement if necessary, the vibration amplitude and spectrum which the payload can be expected to experience. Second, a mechanical model with simulated components should be constructed and then tested for unusual responses to these vibration levels. Third, a specification on the thermal constant, designed to maintain components generally between 0° and 50° C, should be imposed. Fourth, all suppliers should subject their components individually to the expected vibration levels and then to high vacuum tests in which the temperature is cycled 10° C above and below the payload design values. In the cycling, it is just as important to maintain the extremes of temperature for long periods of time as it is to cycle. Finally, the prototype should be assembled and then subjected to 1.5 times the flight vibration levels and to the vacuum-temperature tests. Components which fail the first time should then be tested separately before proceeding with the tests.

For flight units suppliers should construct two sets of components. The "spare" component should receive the flight vibration levels and vacuum temperature testing. The other set of components can be placed into the flight model and then subjected to flight levels and vacuum temperature testing.

## ACKNOWLEDGMENTS

In addition to the authors, the ionospheric experimenters were J. A. Kane and G. P. Serbu. The experimenters for the micrometeorite experiments were W. M. Alexander, O. E. Berg, and C. W. McCracken. W. J. Archer designed the electric field meter instrumentation; C. R. Hamilton acted as Project Coordinator. The following personnel provided the instrumentation: D. S. Hepler (transmitter and command receiver); J. C. Schaffert (command program); J. S. Albus (aspect); D. H. Schaefer (aspect and RF probe